

# Asymmetric gibberellin signaling regulates vacuolar trafficking of PIN auxin transporters during root gravitropism

Christian Löffke<sup>a,1</sup>, Marta Zwiewka<sup>b,c</sup>, Ingo Heilmann<sup>d</sup>, Marc C. E. Van Montagu<sup>b,2</sup>, Thomas Teichmann<sup>a,2</sup>, and Jiří Friml<sup>b,c,e</sup>

<sup>a</sup>Department of Plant Cell Biology, Albrecht-von-Haller-Institute of Plant Sciences, Georg-August University Göttingen, 37077 Göttingen, Germany; <sup>b</sup>Department of Plant Systems Biology, VIB and Department of Plant Biotechnology and Bioinformatics, Ghent University, 9052 Gent, Belgium; <sup>c</sup>Department of Functional Genomics and Proteomics, Central European Institute of Technology, Masaryk University, 625 00 Brno, Czech Republic; <sup>d</sup>Department of Cellular Biochemistry, Institute for Biochemistry and Biotechnology, Martin-Luther-University Halle-Wittenberg, 06120 Halle, Germany; and <sup>e</sup>Institute of Science and Technology Austria, 3400 Klosterneuburg, Austria

Contributed by Marc C. E. Van Montagu, January 9, 2013 (sent for review October 31, 2012)

**Gravitropic bending of plant organs is mediated by an asymmetric signaling of the plant hormone auxin between the upper and lower side of the respective organ. Here, we show that also another plant hormone, gibberellic acid (GA), shows asymmetric action during gravitropic responses. Immunodetection using an antibody against GA and monitoring GA signaling output by downstream degradation of DELLA proteins revealed an asymmetric GA distribution and response with the maximum at the lower side of gravistimulated roots. Genetic or pharmacological manipulation of GA levels or response affects gravity-mediated auxin redistribution and root bending response. The higher GA levels at the lower side of the root correlate with increased amounts of PIN-FORMED2 (PIN2) auxin transporter at the plasma membrane. The observed increase in PIN2 stability is caused by a specific GA effect on trafficking of PIN proteins to lytic vacuoles that presumably occurs downstream of brefeldin A-sensitive endosomes. Our results suggest that asymmetric auxin distribution instructive for gravity-induced differential growth is consolidated by the asymmetric action of GA that stabilizes the PIN-dependent auxin stream along the lower side of gravistimulated roots.**

hormone cross-talk | protein stability | protein trafficking

**D**irectional growth as a response to light or gravity (i.e., tropisms) is a key adaptation response adjusting plant growth to the environment. Tropisms are accomplished by asymmetric elongation of cells within responding organs, which is mediated by differential distribution of the signaling molecule auxin (1). Following a gravitropic stimulus, the intercellular transport of auxin is redirected toward the lower sides of organs, where, in the stem, the higher auxin concentration stimulates cell elongation causing upward bending and, in roots, high auxin concentrations inhibit elongation; as a consequence, roots bend downward (2). The directional cell-to-cell auxin transport depends on the activity of AUXIN RESISTANT1 (AUX1) influx (3) and PIN efflux transporters (4), as well as on auxin transporters from the ATP BINDING CASSETTE SUBFAMILY B (ABCB) family (5). The directionality of auxin flow is determined by polarity of PIN subcellular localization at the plasma membrane (PM) (6, 7). A mechanism for initial redirection of auxin fluxes involves gravity-induced changes in the polarity of PIN localization as observed for PIN3 in root columella (8–10) or shoot endodermis cells (11). The initial auxin asymmetry is further propagated from the root tip by asymmetric degradation of PIN2 at the upper vs. the lower side of the gravistimulated root (12, 13).

PIN proteins undergo constitutive subcellular dynamics involving endocytic recycling to different domains at the PM or re-routing via the prevacuolar compartment to the lytic vacuole for degradation (12–15). Thus, PIN abundance can be regulated by changes in trafficking or transcription (16). Several other hormonal

signaling pathways have been shown to affect directionality and throughput of PIN-dependent auxin fluxes. These include feedback regulation of PIN internalization (17, 18) and polarity (19) by auxin; brassinosteroid (20), cytokinin (21, 22), and ethylene (23, 24) effects on PIN transcription; as well as cytokinin effects on PIN degradation (25). Moreover, gibberellin biosynthesis mutants show increased PIN degradation (26).

With respect to the gravitropism, the main focus of the previous research has been on auxin and, in particular, its asymmetric distribution. However, in some monocot species, including rice, maize, and barley, asymmetric accumulation of auxin and gibberellic acid (GA) at the lower side of gravistimulated organs has been reported (27–29), but general validity and physiological significance of these observations remain unclear.

Here, we show an asymmetric distribution of GA and GA signaling during root gravitropic growth. Furthermore, we observed that GA increases the levels of PIN auxin transporters at the PM by inhibiting PIN vacuolar trafficking. These observations suggest that an interplay between asymmetric auxin and gibberellin activities modulates and stabilizes auxin fluxes for root gravitropic responses.

## Results and Discussion

**Gravity Stimulation Induces Asymmetric GA Distribution and Response.** To test for a role of GA in root gravitropism in *Arabidopsis thaliana*, we examined GA distribution following gravistimulation. As direct measurements of GA distributions are technically not feasible in intact *Arabidopsis* roots, we established a whole-mount immunodetection of GA in *Arabidopsis* root tips by using an antibody raised against BSA-conjugated GA (for details see *Materials and Methods*). Control experiments showed specific binding of the anti-GA antibody to the epidermal cells of cell division and elongation zones of the root tip (Fig. S1 A–G). Much weaker anti-GA signals were detected in the seedlings in which GA production was inhibited genetically in the *ga1-3* mutant (30) or pharmacologically by uniconazole (Uni) treatment (31) (Fig. S1 H–J), confirming that a specific labeling of GA had been detected. As our immunolocalization method is only reliable for root tips (32), we cannot assess the GA distribution in the more differentiated parts of the root or make

Author contributions: I.H., M.C.E.V.M., T.T., and J.F. designed research; C.L. and M.Z. performed research; C.L. and M.Z. analyzed data; and C.L., T.T., and J.F. wrote the paper.

The authors declare no conflict of interest.

<sup>1</sup>Present address: Department of Applied Genetics and Cell Biology, University of Applied Life Sciences and Natural Resources, 1190 Vienna, Austria.

<sup>2</sup>To whom correspondence may be addressed. E-mail: tteichm@gwdg.de or marc.vanmontagu@ugent.be.

This article contains supporting information online at [www.pnas.org/lookup/suppl/doi:10.1073/pnas.1300107110/-DCSupplemental](http://www.pnas.org/lookup/suppl/doi:10.1073/pnas.1300107110/-DCSupplemental).

a quantitative comparison between different root tissues such as endodermis, in which GA is important to control root growth (33). Following gravistimulation, the originally symmetric GA labeling became asymmetric with markedly stronger signal at the lower side of the root and a weaker signal at the upper side after approximately 3 h (Fig. 1 A–C). This result suggests that gravity induces asymmetry in GA distribution in gravistimulated root tips.

To verify the antibody-based observations, we analyzed downstream GA responses following gravistimulation. GA promotes degradation of downstream regulators, the DELLA proteins, which depends on cellular GA concentrations (34). Thus, quantitative analysis of the GFP-tagged DELLA protein REPRESSOR OF GA1-3 (RGA) in *RGA::GFP-RGA* seedlings allows monitoring of the GA response in plant tissues. We observed a significant ( $P \leq 0.05$ ) decrease of the GFP-RGA signal at the lower side of the root tip approximately 3 h after gravistimulation (Fig. 1 D–F). This reflects an increase in GA response at the lower side of the root and is entirely consistent with increased anti-GA signals there. In summary, GA immunodetection and GA response monitoring revealed asymmetric GA distribution with higher GA levels at the lower side of the gravistimulated roots.

Our data reveal that not only auxin (35, 36) but also GA shows an asymmetric distribution in the gravistimulated root tips. To compare the kinetics of these events, we monitored the expression of GA-responsive *GA20ox1* (37) and auxin-responsive *GH3.1* genes (38). Following gravitropic stimulation, *GA20ox1* expression showed gradual up-regulation (Fig. S2), whereas the

*GH3.1* gene showed faster but transient up-regulation of expression (Fig. S2). Consistently, gravity-induced auxin response asymmetry as monitored by the *DR5rev::GFP* (35) or DII-Venus (36) reporters was established faster than the observed GA asymmetry, suggesting a chronological order of changes in hormone responses during gravitropism, whereby GA asymmetry develops only after the initial auxin asymmetry establishment.

**GA Action Is Required for Root Gravitropism and Asymmetric Auxin Distribution.** Asymmetry in GA distribution during gravitropism implies that GA plays a role in root gravitropic responses that was also suggested by gravitropic defects in GA biosynthesis mutants (26). Therefore, we studied the consequences of manipulating GA levels and GA signaling on root gravitropism in *Arabidopsis*. Treatment with the GA biosynthesis inhibitor uniconazole, as well as GA depletion in the GA biosynthetic *gai-3* mutant (30) or inhibition of GA signaling in the dominant-negative DELLA mutant *gaiΔ17* (39), consistently caused defects in gravitropic root bending (Fig. 2 A and B). Effects of increased GA signaling were analyzed in seedlings treated with exogenous GA and the *Arabidopsis pentuple* mutant carrying lesions in all five DELLA repressors acting downstream of GA (40). Also, these treatments and mutants showed a defect in root gravitropism (Fig. 2 A and B), confirming that manipulation of GA levels and signaling reduce the root gravitropic response.

Root gravitropic bending is accompanied by asymmetric auxin distribution and response with the maximum at the lower side of gravistimulated roots (35, 36) that is disrupted in GA biosynthesis mutants (26). This asymmetry can be monitored with auxin response reporters such as *DR5rev::GFP* (41, 42) showing increased activity at the lower side of the root (Fig. 2C). Positive (i.e., GA treatment) and negative (i.e., uniconazole treatment) manipulations of GA levels interfered with the establishment of the asymmetric auxin response in the root tip following gravistimulation. Roots treated with GA showed a symmetrically increased signal in the lateral root cap that was not detected in nontreated roots (Fig. 2 C and D). On the contrary, inhibition of GA biosynthesis by uniconazole prevented lateral accumulation of the *DR5rev::GFP* signal (Fig. 2E). These analyses show that balanced levels of GA are required for gravity-induced asymmetric auxin responses and for root gravitropic growth.

**GA Acts on Root Gravitropism by Regulating Levels of PIN Auxin Transporters.** Next, we assessed a possible mechanism by which GA interferes with auxin distribution and root gravitropism. Gravity-induced auxin redistribution requires directional activity of PIN auxin transporters (4, 6), of which loss-of-function (*pin2/eir1*) (43) and gain-of-function (*35S::PIN1*) (4, 44) alleles show root agravitropic phenotypes. Notably, interfering with GA biosynthesis by uniconazole treatment amplified *pin2* defects (Fig. S3), but largely normalized the severe agravitropic phenotype of *35S::PIN1* roots (Fig. 3B). Similarly, inhibiting GA signaling in the dominant-negative DELLA mutant *gaiΔ17* (39) rescued normal gravitropic growth in *35S::PIN1* × *gaiΔ17* double-mutant lines (Fig. 3C). These effects of GA on *pin* mutants suggest that GA regulates root gravitropism by a mechanism involving PIN auxin transporters.

The agravitropic phenotype of *35S::PIN1* roots is presumably caused by the ectopic expression of *PIN1* in the root epidermis cells (6, 45). Immunolocalization studies of *35S::PIN1* roots showed a known ectopic presence of *PIN1* in epidermis cells (Fig. 3F), whereas *gaiΔ17* showed weaker, but overall normal pattern of *PIN1* localization (Fig. 3H). The *35S::PIN1* × *gaiΔ17* double mutant exhibited a strongly decreased ectopic presence of *PIN1* in the epidermis (Fig. 3G), correlating with the rescue of normal gravitropic growth (Fig. 3C). This observation suggests that GA effects on root gravitropism are related to regulation of *PIN* abundance.

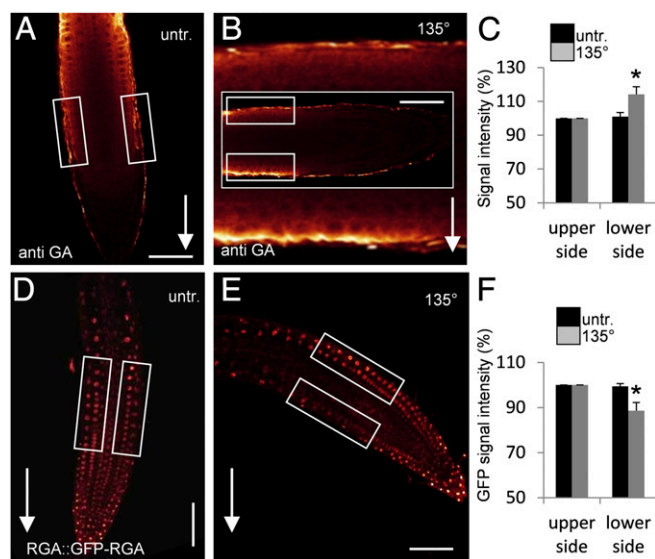


**Fig. 1.** Asymmetric GA distribution and response in gravistimulated *Arabidopsis* roots. (A–C) Detection of asymmetric GA localization in gravitropically induced roots immunostained with a GA-specific antibody. Atto647N conjugated anti-rat/goat was used as secondary antibody. Seedlings were grown vertically (A) or gravitropically induced for 3 h (B). Arrows indicate direction of the gravity vector. The image in the background of B shows enlargement of the root area that was used for quantification; small rectangles specify areas where fluorescence signal intensities of upper and lower side were quantified. (C) Quantification of signals on upper and lower sides of control and gravistimulated roots by image analysis; data represent means  $\pm$  SE ( $n = 8$ ; experiment repeated two times and representative data shown). (D and E) *Arabidopsis RGA::GFP-RGA* seedlings were grown vertically (D) or gravitropically induced for 3 h (E); boxes indicate areas used for quantification of fluorescence signal intensities. (F) Quantification of *RGA::GFP-RGA* signals on upper and lower sides of control and gravistimulated roots by image analysis; data represent means  $\pm$  SE ( $n = 8$ ; experiment repeated three times and representative data shown). \* $P \leq 0.05$  upper vs. lower side. (Scale bars: A, B, D, and E, 50  $\mu$ m.)

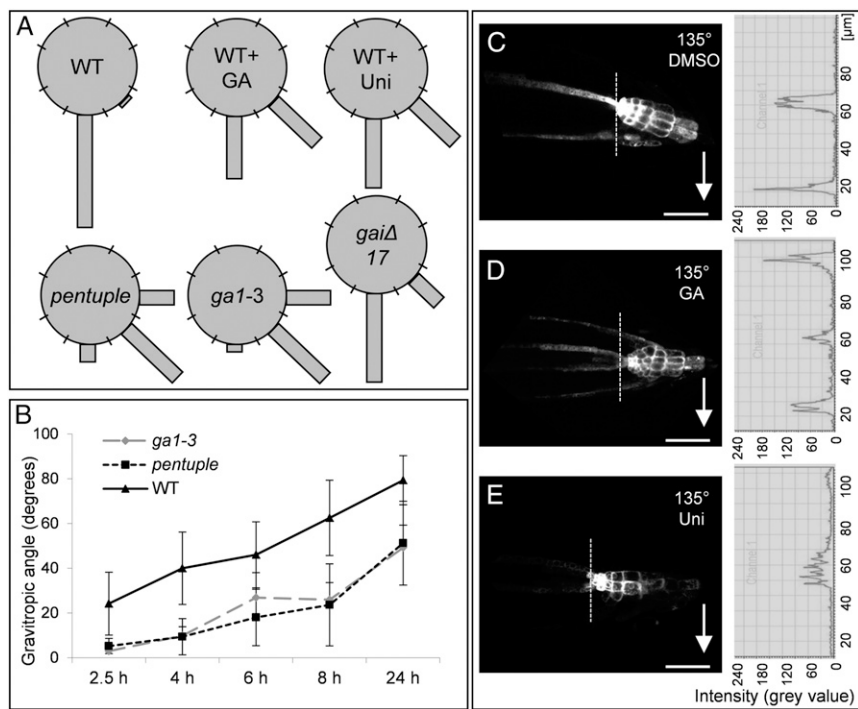


**Fig. 2.** Requirement of balanced GA levels and signaling for root gravitropism. (A) Pharmacological treatments and analysis of GA biosynthesis and signaling mutants have been used to study GA effects on gravitropism. Gravistimulated roots were assigned to one of the eight 45° sectors on a gravitropism diagram. The length of bars in the diagram represents percentage of seedlings assigned to the respective sector. (B) The time course of root reorientation after gravistimulation was recorded in the *ga1-3* and the *pentuple* mutant in comparison with WT seedlings. Data represent means  $\pm$  SD ( $n = 8$  seedlings per treatment, experiments repeated three times, representative data shown). (C–E) *Arabidopsis DR5rev::GFP* seedlings pretreated with DMSO (GA and uniconazole solvent) (C), 50  $\mu$ M GA for 3 h (D), or 10  $\mu$ M uniconazole for 2 d (E), and subsequently gravitropically induced for 1.5 h. Graphs show fluorescence profiles of the root tip; the profile represents fluorescence intensities across a sector measured above the quiescent center (dotted line); arrows mark direction of the gravity vector. (Scale bar: 50  $\mu$ m.)

**GA Increases PIN Protein Stability by Inhibiting PIN Vacuolar Trafficking.**

High GA levels detected at the lower side of gravistimulated roots (Fig. 1) correlate with higher PIN2 abundance there (12, 35). In addition, the GA-deficient *ga1-3* mutant has been shown to have lower PIN2 levels (26). GA does not change *PIN2* gene expression (Fig. S4). This, together with the decreased ectopic *PIN1* expression under conditions of inhibited GA signaling in *35S::PIN1*  $\times$  *gaiΔ17* roots (Fig. 3G), suggests that GA inhibits turnover of PIN proteins. To test the effect of increased GA levels on PIN2 protein amounts independently of *PIN* transcription, we analyzed PIN2 turnover in *TA::PIN2-GFP* plants (12) that allow dexamethasone (DEX)-inducible expression of *PIN2*. After induction of *PIN2* expression in a *TA::PIN2-GFP* line for 24 h, DEX was washed out and seedlings were treated with GA or with DMSO as a control. The GA treatment dramatically increased PIN2 stability compared with untreated controls (Fig. 4 A–C).

To investigate if this GA effect is specific for PIN proteins, we tested for differences in the PM amounts of the auxin influx

carrier AUX1 (46), the auxin transporter P-glycoprotein19 (PGP19/ABCB19) (47), and the aquaporin PLASMALEMMA INTRINSIC PROTEIN2 (PIP2) (48), and found that they were not influenced by GA or the GA biosynthesis inhibitor paclobutrazol (31) (Fig. S5 A–Q). In contrast, all *Arabidopsis* PM PIN proteins—PIN1-GFP (44), PIN2-GFP (12), PIN3-GFP (49), PIN4-GFP (50), and PIN7-GFP (10)—showed increased and decreased signals after GA and paclobutrazol treatments, respectively (Fig. S5 R–T). These data indicate that GA specifically influences the stability of PIN proteins.

The PIN2 protein amount at the PM is regulated by a balance between vacuolar trafficking-mediated degradation and constitutive recycling back to the PM (14). Trafficking of PIN2-GFP to the lytic vacuole can be visualized by moving plants to dark, leading to accumulation of detectable GFP in the vacuoles (51). In line with previous observations (13), *PIN2::PIN2-GFP* plants kept in the dark showed a prominent GFP signal in intracellular compartments in addition to the PM signal (Fig. 4G). These

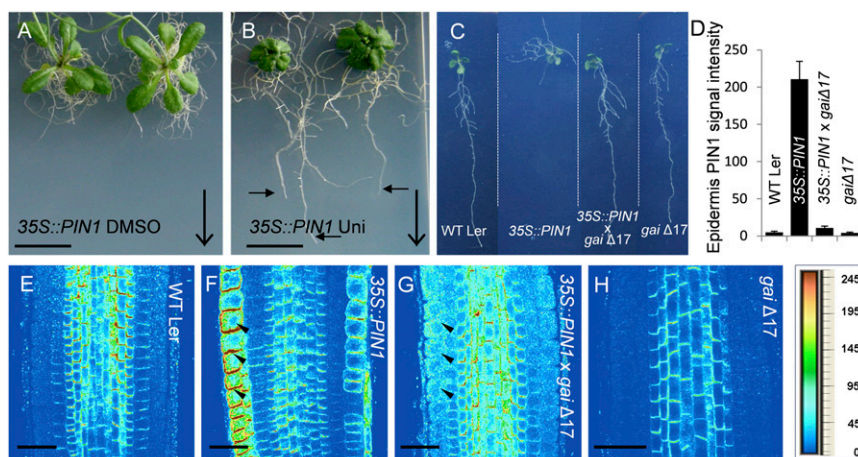


**Fig. 3.** GA effects on PIN-mediated root gravitropism. *35S::PIN1* were germinated on one-half MS medium and subsequently sprayed with DMSO (A) or 10  $\mu$ M uniconazole (B). Images were taken 2 wk after start of treatments. Large arrows indicate direction of the gravity vector and small arrows indicate root growth along the gravity vector after treatment. *gaiΔ17* was introgressed into *35S::PIN1* background, and root growth and immune stainings analysis were performed. (C) Root growth of WT Landsberg *erecta* (Ler), *35S::PIN1*, *35S::PIN1*  $\times$  *gaiΔ17*, and *gaiΔ17* seedlings is shown. (D–H) Immunolocalization of PIN1 was done in root tips of (E) WT Ler seedlings, (F) *35S::PIN1*, (G) *35S::PIN1*  $\times$  *gaiΔ17*, and (H) *gaiΔ17*. Quantification of PIN1 signals in the root epidermis (E–H) is shown in D. Arrowheads indicate ectopic localization of PIN1 in the PIN1 overexpression line (F). Heat map provides a color code of fluorescence signal intensities shown in E–H. (Scale bars: A and B, 1 cm; E–H, 30  $\mu$ m.)

GFP-labeled intracellular compartments were identified as vacuoles by experiments that used the endocytic tracer FM4-64 (52). *PIN2::PIN2-GFP* plants were kept for 4 h in the dark and stained for 1 h with FM4-64 to visualize the tonoplast membranes. Overlay of GFP and FM4-64 fluorescence images showed GFP signal in the vacuolar lumen (Fig. S6 A–C). In these experiments, GA treatment resulted in a dramatic decrease of the vacuolar signal, whereas the PIN2-GFP PM signal was notably increased

(Fig. 4 D, G, and H). Also, Western blot analysis showed an increase of PIN2 protein abundance in GA-treated roots (Fig. 4F). A complementary experiment in uniconazole-treated plants revealed that low GA levels increase the amount of the GFP signal in the lytic vacuoles (Fig. 4 E, I, and J) consistent with previous reports (26). Together, these experiments show that GA increases stability specifically of PIN proteins by regulating the rate of PIN trafficking into the lytic vacuole, a process inhibited by high and promoted by low GA levels.

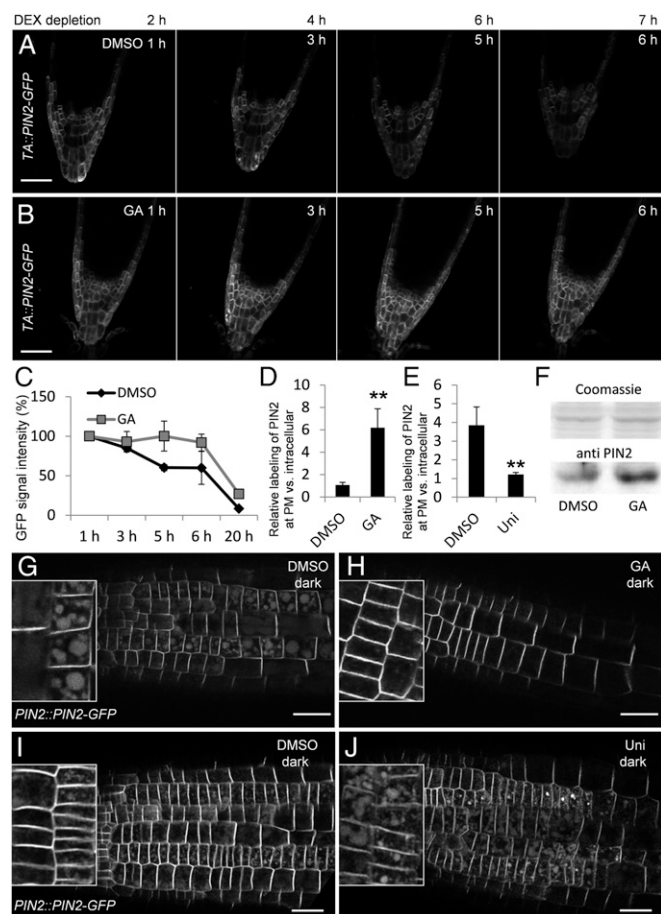


**Fig. 4.** GA effects on PIN stability and vacuolar trafficking. (A and B) *PIN2* expression was induced in *TA::PIN2-GFP* seedlings by treatment with 30  $\mu$ M DEX for 24 h. After depletion of DEX by washing, roots were mounted with or without GA and *PIN2-GFP* signal intensities were recorded after the indicated time points. Roots were treated with DMSO as control (A) or with 50  $\mu$ M GA (B). To rule out that the DEX-inducible promoter responds to GA, *TA::PIN2-GFP* seedlings were treated for 24 h with GA without DEX, but did not show induction of *PIN2-GFP* expression. To have a strong *PIN2-GFP* signal for quantification, root columella cells were imaged. (C) Total *PIN2-GFP* signal intensity at time point 1 h DMSO and GA, respectively, was set to 100%, and relative signal intensity of subsequent time points was calculated as percentage of total signal intensity at time point 1 h. (D and E) *PIN2-GFP* signal at the PM relative to intracellular signal after GA treatment (D) and after uniconazole treatment (E). A small box of the size of the PM signal was used to define the region of interest for the PM quantification; the intracellular signal was quantified within a rectangle region of interest covering the cell volume. The ratio of PM vs. internal signal was measured in seven cells in a row ( $n = 8$  individual roots). \*\* $P \leq 0.01$ . (F) Western Blot analysis of roots treated for 3 h with DMSO or 50  $\mu$ M GA. (G–J) Vacuolar targeting of *PIN2* was analyzed after treatment [GA and uniconazole (Uni)] of seedlings in the light and then transferred to the dark for 6 h (G and H) or 3 h (I and J). *PIN2::PIN2-GFP* seedlings were pretreated with DMSO (GA solvent) for 3 h (G), 50  $\mu$ M GA for 3 h (H), DMSO (uniconazole solvent) for 2 d (I), or 10  $\mu$ M uniconazole for 2 d (J). (Scale bars: A and B, 50  $\mu$ m; G–J, 25  $\mu$ m.)

#### GA Targets PIN Vacuolar Trafficking Downstream of BFA-Sensitive Endosomes.

The data so far raised the question at what particular PIN trafficking step GA acts to regulate PIN turnover. Uptake experiments with the endocytosis marker FM4-64 in *gal-3* and *pentuple* mutants and in seedlings treated with GA or uniconazole did not show any differences vs. untreated WT controls (Fig. S7A), not supporting a notion that GA acts on endocytosis.

Following endocytosis, PIN proteins are sorted in the endosomes for recycling back to the PM or for further trafficking toward the vacuole (14). The recycling and, to a lesser extent, vacuolar trafficking are sensitive to the vesicle trafficking inhibitor brefeldin A (BFA) (13, 35). BFA treatment aggregates different types of endosomes and thus allows better visualization of the endosomal and vacuolar trafficking cargoes, including PIN proteins (35, 53). GA treatment preceding BFA application increased (Fig. 5 A–C)—whereas low GA levels in uniconazole-treated roots or in the *gal-3* mutant decreased—the *PIN2-GFP* signal in BFA-induced aggregates compared with controls (Fig. 5 D–I). This suggests that high GA promotes and low GA inhibits PIN retrograde trafficking somewhere downstream of the BFA-sensitive endosomes. A contrasting outcome was seen in similar experiments with another trafficking inhibitor, wortmannin (WM), that leads to swelling and aggregation of prevacuolar compartments (13, 54). We did not observe any change of the *PIN2-GFP* accumulation in WM-induced intracellular aggregations with increased (i.e., GA treatment) or decreased (i.e., uniconazole treatment, *gal-3* mutant) GA levels (Fig. S7B).

In summary, these experiments with the use of different markers and trafficking inhibitors confirmed that GA interferes with vacuolar trafficking of PIN proteins. GA targets presumably a trafficking step downstream of BFA-sensitive endosomes toward the vacuole.

#### Conclusion

PM proteins targeted for degradation are endocytosed and subsequently hydrolyzed by proteases in the lytic vacuole after a passage through the early and late endosomes. During gravitropism, the *PIN2* auxin transporter is degraded at the upper side of the root and stabilized at the lower root side, thus contributing to the asymmetric auxin flow that mediates gravitropic bending (12, 13, 35). The *PIN2* destabilization at the upper side is mediated by the low auxin levels and signaling (35), and the initial increase of *PIN2* levels at the lower side is presumably caused by auxin-mediated inhibition of *PIN2* endocytosis (18). Here, we propose an additional or alternative mechanism for *PIN2* stabilization at the lower side. We detected asymmetry of another plant signaling molecule, GA, in gravistimulated roots with high GA levels at the lower side. GA also stabilizes specifically *PIN2* proteins by inhibiting their trafficking to the lytic vacuole, providing the possibility that GA contributes to the stabilization of *PIN2* at the lower side of the root and, thus, promotes asymmetric auxin flow and distribution for gravitropic bending. In line with this hypothesis, interference with GA levels or signaling modifies the gravity-induced asymmetric auxin response and gravitropic bending. On the contrary, GA asymmetry appears to develop only after the initial gravity-induced auxin asymmetry, suggesting mutual feed-back regulation of these two pathways. Based on these different kinetics, auxin may control the early

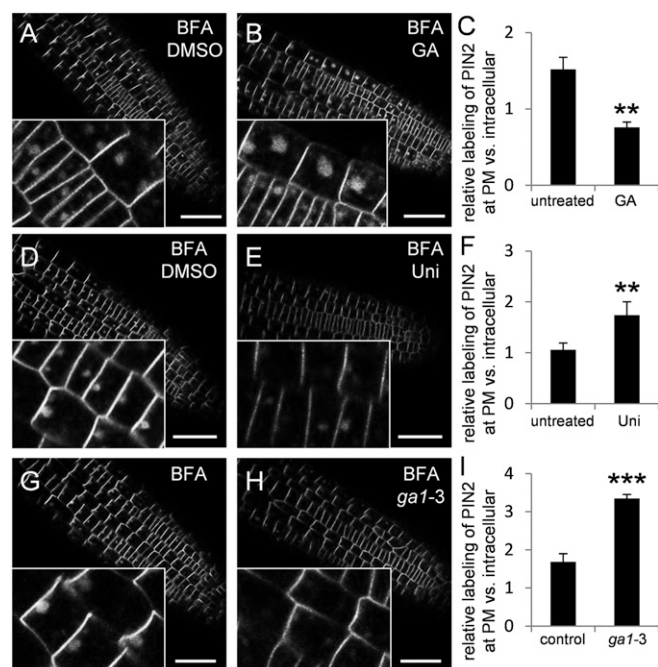


**Fig. 5.** GA inhibition of vacuolar PIN trafficking downstream of BFA action. The PIN2::PIN2-GFP signal in BFA endosomes was imaged after treatment with DMSO for 3 h (GA control) (A), 50  $\mu$ M GA for 3 h (B), DMSO for 2 d (uniconazole control) (D), or 10  $\mu$ M uniconazole for 2 d (E). (G and H) PIN2-GFP signal in BFA endosomes of (G) *PIN2::PIN2-GFP* and (H) *PIN2::PIN2-GFP* × *ga1-3* seedlings. (C, F, and I) Quantification of PIN2-GFP signal at the PM relative to endosomal signals in seedlings treated as described in A, B, D, E, G, and H. Data represent means  $\pm$  SD ( $n = 7$  roots were analyzed per treatment, and, in six cells per root, endosomal signal was quantified; \* $P \leq 0.05$ , \*\* $P \leq 0.01$ , and \*\*\* $P \leq 0.001$ , treatment vs. control). (Scale bar: 50  $\mu$ m.)

response of the root to a gravitropic stimulus and GA subsequently maintains gravitropic curvature by stabilizing the PIN-dependent auxin stream along the lower side of the root. The emerging picture involves GA as a part of the complex network consolidating asymmetric auxin action during gravitropic responses and, possibly, also other auxin-mediated processes, as suggested by GA requirement for auxin-mediated organ formation (26).

## Materials and Methods

**Lines.** The *pentuple* mutant (40) was obtained from the Nottingham *Arabidopsis* Stock Centre (ID N16298). *ga1-3* (55), *gai17* (39), *35S::PIN2-GFP* (56), *35S::PIN1* (44), *DR5rev::GFP* (42), *AUX1::AUX1-YFP* (57), *PIN2::PIN2-GFP* (12), *pin2/air1* (43), *PIN3::PIN3-GFP* (49), *PIN4::PIN4-GFP* (50), *PIN7::PIN7-GFP* (42), *PGP19::PGP19-GFP* (45), *RGA::GFP-RGA* (34), and *TA::PIN2-GFP* (12) were described previously. Combinations of mutations and reporter lines were obtained by crossing individual lines. As the GA mutants are in the accession *Landsberg erecta*, this ecotype was used as control for analysis of the GA mutants.

**Growth Conditions.** Seeds were surface sterilized with 70% (vol/vol) ethanol supplemented with 0.05% Tween and dried on sterile filter paper. Plants were grown vertically on one-half Murashige and Skoog (MS) medium, including vitamins (Duchefa), with 1% sucrose and 0.5 g/L Mes (pH 5.7), under a 16 h light/8 h dark photoperiod at 22/18 °C. All experiments were carried out in the light period including the dark treatments. Gravitropic experiments were performed as previously described (8); detailed information is provided in *S1 Materials and Methods*.

**Pharmacological Treatments and Experimental Conditions.** Chemicals were applied in solid or liquid MS medium or by spraying 7-d-old seedlings with BFA [50 mM stock in ethanol; final concentration (f.c.) 50  $\mu$ M], DEX (30 mM stock in DMSO; f.c. 30  $\mu$ M), FM4-64 (2 mM stock in DMSO; f.c. 2  $\mu$ M), GA<sub>3</sub> (100 mM stock in DMSO; f.c. 50  $\mu$ M), uniconazole (10 mM stock in DMSO; f.c. 10  $\mu$ M), paclobutrazol (10 mM stock in DMSO; f.c. 10  $\mu$ M), or WVM (10 mM stock in DMSO; f.c. 30  $\mu$ M). Mock treatments were done by using equal amounts of solvent (DMSO), and double treatments were carried out within a 1-h interval. All independent experiments were performed at least in triplicate, with a minimum of eight individual plants. BFA, WM, and FM4-64 were applied in liquid MS medium for 2 h (BFA), 4.5 h (WVM), and 1 h (FM4-64).

Dark treatments were done as described previously (13). To compare protein concentrations in the lytic vacuole, epidermal cells at the interface of the meristematic and elongation zone were recorded. For live cell GFP imaging, a Leica DM6000 CS, TCS SP5 AOBs confocal laser scanning microscope was used, and fluorescent signals were quantified by using the integrated Leica quantification module (LAS AF 2.1.0). Fluorescent measurements were done on the original Leica image files. Representative images are shown. Statistics were evaluated with GraphPad QuickCalcs *t* test (<http://graphpad.com/quickcalcs/index.cfm>).

**Immunodetection of GA in Roots and Competition Assays.** Whole-mount immunolocalization was done as described previously (58) after a prefixation step using a freshly prepared 3% *N*-ethyl-*N'*-(3-dimethylaminopropyl) carbodiimide hydrochloride (Sigma) solution in PBS solution for 1 h (44). Antibodies were diluted as follows: 1:100 BSA (Agrisera), 1:200 DyLight 488 (Agrisera), 1:100 anti-GA<sub>3</sub> (Agrisera), and 1:150 for Atto647N-conjugated anti-rat/goat (provided by Stefan Jakobs, Max Planck Institute for Biophysical Chemistry, Göttingen, Germany). Antibody depletion experiments to identify GA-specific signals were carried out with GA<sub>3</sub>-BSA conjugate obtained from Agrisera. Anti-GA antibody and GA<sub>3</sub>-BSA conjugate were used in a 1:10 ratio. The setup for antibody depletion was designed with competition calculator from Agrisera. Antibody and GA<sub>3</sub>-BSA conjugate were incubated in 1× PBS solution (24 h, 4 °C, rotator) in a total volume of 225  $\mu$ L and then used as a primary antibody for immunodetection of GA in paraformaldehyde-fixed and BSA-blocked root samples. In parallel, non-depleted serum was used to differentiate between GA-specific and non-specific signals in the immunolocalization experiments. To distinguish between the upper and lower side after gravistimulation, we coexpressed *DR5rev::GFP* or used the already established bending of the root for orientation. The immunodetection of GA was done in independent triplicates repeated with eight individual plants. The competition assay with the GA<sub>3</sub>-BSA conjugate was performed twice with eight individual plants.

**Immunodetection of PIN Proteins in Roots.** Automated whole mount protein immunolocalization was done as described previously (32). The anti-PIN1 rabbit antibody (18) was used at a dilution of 1:500. The whole-mount protein immunolocalization was repeated three times.

**DEX Depletion Assay.** *TA::PIN2-GFP* seedlings were grown on solid one-half MS for 6 d and transferred to 30  $\mu$ M DEX-supplemented solid one-half MS media for 24 h. After washing three times for 20 min in liquid one-half MS without sucrose, the roots were mounted in 3% glycerine with 50  $\mu$ M GA<sub>3</sub> or equal amount of GA solvent, and PIN2-GFP signal was recorded after 2, 4, 6, 7, and 24 h. To estimate the possible induction of the inducible DEX promoter by GA, the *TA::PIN2-GFP* line was transferred to only GA (50  $\mu$ M)-supplemented solid one-half MS media for 24 h and recorded. The experiment was performed in triplicate with a minimum of five individual plants.

**ACKNOWLEDGMENTS.** We thank Volker Lipka for providing the infrastructure of his department; Alexandra Matei, Charlotte Roth, Mena Erkenschwick, and Sören Rindfleisch for their contribution to the project; Joanna Porankiewicz-Asplund (Agrisera) for support in the characterization of the anti-GA antibody; and Stefan Jakobs for providing the Atto647N conjugated anti-rat/goat antibody. This research was supported by Deutsche Forschungsgemeinschaft Grant ERA-PD 045 and Central European Institute of Technology Project CZ.1.05/1.1.0/02/0068 from the European Regional Development Fund.

- Muday GK, Rahman A (2007) *Plant Tropisms*, eds Gilroy S, Masson PH (Wiley, Chichester, UK), pp 46–77.
- Tanimoto E (2005) Regulation of root growth by plant hormones—Roles for auxin and gibberellin. *Crit Rev Plant Sci* 24(4):249–265.

- Yang Y, Hammes UZ, Taylor CG, Schachtman DP, Nielsen E (2006) High-affinity auxin transport by the AUX1 influx carrier protein. *Curr Biol* 16(11):1123–1127.
- Petrásek J, et al. (2006) PIN proteins perform a rate-limiting function in cellular auxin efflux. *Science* 312(5775):914–918.

5. Geisler M, et al. (2005) Cellular efflux of auxin catalyzed by the Arabidopsis MDR/PGP transporter AtPGP1. *Plant J* 44(2):179–194.
6. Wiśniewska J, et al. (2006) Polar PIN localization directs auxin flow in plants. *Science* 312(5775):883.
7. Zhang J, Nodzyński T, Pěncík A, Rolčík J, Friml J (2010) PIN phosphorylation is sufficient to mediate PIN polarity and direct auxin transport. *Proc Natl Acad Sci USA* 107(2):918–922.
8. Friml J, Wiśniewska J, Benková E, Mendgen K, Palme K (2002) Lateral relocation of auxin efflux regulator PIN3 mediates tropism in Arabidopsis. *Nature* 415(6873):806–809.
9. Harrison BR, Masson PH (2008) ARL2, ARG1 and PIN3 define a gravity signal transduction pathway in root statocytes. *Plant J* 53(2):380–392.
10. Kleine-Vehn J, et al. (2010) Gravity-induced PIN transcytosis for polarization of auxin fluxes in gravity-sensing root cells. *Proc Natl Acad Sci USA* 107(51):22344–22349.
11. Rakusová H, et al. (2011) Polarization of PIN3-dependent auxin transport for hypocotyl gravitropic response in Arabidopsis thaliana. *Plant J* 67(5):817–826.
12. Abas L, et al. (2006) Intracellular trafficking and proteolysis of the Arabidopsis auxin-efflux facilitator PIN2 are involved in root gravitropism. *Nat Cell Biol* 8(3):249–256.
13. Kleine-Vehn J, et al. (2008) Differential degradation of PIN2 auxin efflux carrier by retromer-dependent vacuolar targeting. *Proc Natl Acad Sci USA* 105(46):17812–17817.
14. Kleine-Vehn J, Friml J (2008) Polar targeting and endocytic recycling in auxin-dependent plant development. *Annu Rev Cell Dev Biol* 24:447–473.
15. Löffke C, Luschnig C, Kleine-Vehn J (2013) Posttranslational modification and trafficking of PIN auxin efflux carriers. *Mech Dev* 130(1):82–94.
16. Grunewald W, Friml J (2010) The march of the PINs: Developmental plasticity by dynamic polar targeting in plant cells. *EMBO J* 29(16):2700–2714.
17. Robert S, et al. (2010) ABP1 mediates auxin inhibition of clathrin-dependent endocytosis in Arabidopsis. *Cell* 143(1):111–121.
18. Paciorek T, et al. (2005) Auxin inhibits endocytosis and promotes its own efflux from cells. *Nature* 435(7046):1251–1256.
19. Sauer M, et al. (2006) Canalization of auxin flow by Aux/IAA-ARF-dependent feedback regulation of PIN polarity. *Genes Dev* 20(20):2902–2911.
20. Nakamura A, Goda H, Shimada Y, Yoshida S (2004) Brassinosteroid selectively regulates PIN gene expression in Arabidopsis. *Biosci Biotechnol Biochem* 68(4):952–954.
21. Růžicka K, et al. (2009) Cytokinin regulates root meristem activity via modulation of the polar auxin transport. *Proc Natl Acad Sci USA* 106(11):4284–4289.
22. Moubayidin L, et al. (2010) The rate of cell differentiation controls the Arabidopsis root meristem growth phase. *Curr Biol* 20(12):1138–1143.
23. Růžicka K, et al. (2007) Ethylene regulates root growth through effects on auxin biosynthesis and transport-dependent auxin distribution. *Plant Cell* 19(7):2197–2212.
24. Swarup R, et al. (2007) Ethylene upregulates auxin biosynthesis in Arabidopsis seedlings to enhance inhibition of root cell elongation. *Plant Cell* 19(7):2186–2196.
25. Marhavý P, et al. (2011) Cytokinin modulates endocytic trafficking of PIN1 auxin efflux carrier to control plant organogenesis. *Dev Cell* 21(4):796–804.
26. Willige BC, Isono E, Richter R, Zourelidou M, Schwechheimer C (2011) Gibberellin regulates PIN-FORMED abundance and is required for auxin transport-dependent growth and development in Arabidopsis thaliana. *Plant Cell* 23(6):2184–2195.
27. Cui D, Neill SJ, Tang Z, Cai W (2005) Gibberellin-regulated XET is differentially induced by auxin in rice leaf sheath bases during gravitropic bending. *J Exp Bot* 56(415):1327–1334.
28. Rood SB, Kaufman PB, Abe H, Pharis RP (1987) Gibberellins and gravitropism in maize shoots: Endogenous gibberellin-like substances and movement and metabolism of [<sup>3</sup>H]gibberellin A<sub>20</sub>. *Plant Physiol* 83(3):645–651.
29. Wolbang CM, Davies NW, Taylor SA, Ross JJ (2007) Gravitropism leads to asymmetry of both auxin and gibberellin levels in barley pulvini. *Physiol Plant* 131(1):140–148.
30. Sun T-P, Kamiya Y (1994) The Arabidopsis GA1 locus encodes the cyclase ent-kaurene synthetase A of gibberellin biosynthesis. *Plant Cell* 6(10):1509–1518.
31. Rademacher W (2000) Growth retardants: Effects on gibberellin biosynthesis and other metabolic pathways. *Annu Rev Plant Physiol Plant Mol Biol* 51:501–531.
32. Sauer M, Paciorek T, Benková E, Friml J (2006) Immunocytochemical techniques for whole-mount in situ protein localization in plants. *Nat Protoc* 1(1):98–103.
33. Ubeda-Tomás S, et al. (2008) Root growth in Arabidopsis requires gibberellin/DELLA signalling in the endodermis. *Nat Cell Biol* 10(5):625–628.
34. Silverstone AL, et al. (2001) Repressing a repressor: Gibberellin-induced rapid reduction of the RGA protein in Arabidopsis. *Plant Cell* 13(7):1555–1566.
35. Baster P, et al. (2013) SCF<sup>(TIR1/AFB)</sup>-auxin signalling regulates PIN vacuolar trafficking and auxin fluxes during root gravitropism. *EMBO J* 32(1):260–274.
36. Band LR, et al. (2012) Root gravitropism is regulated by a transient lateral auxin gradient controlled by a tipping-point mechanism. *Proc Natl Acad Sci USA* 109(12):4668–4673.
37. Phillips AL, et al. (1995) Isolation and expression of three gibberellin 20-oxidase cDNA clones from Arabidopsis. *Plant Physiol* 108(3):1049–1057.
38. Hagen G, Guilfoyle T (2002) Auxin-responsive gene expression: Genes, promoters and regulatory factors. *Plant Mol Biol* 49(3–4):373–385.
39. Peng J, et al. (1997) The Arabidopsis GAI gene defines a signaling pathway that negatively regulates gibberellin responses. *Genes Dev* 11(23):3194–3205.
40. Feng S, et al. (2008) Coordinated regulation of Arabidopsis thaliana development by light and gibberellins. *Nature* 451(7177):475–479.
41. Ulmasov T, Murfett J, Hagen G, Guilfoyle TJ (1997) Aux/IAA proteins repress expression of reporter genes containing natural and highly active synthetic auxin response elements. *Plant Cell* 9(11):1963–1971.
42. Friml J, et al. (2003) Efflux-dependent auxin gradients establish the apical-basal axis of Arabidopsis. *Nature* 426(6963):147–153.
43. Luschnig C, Gaxiola RA, Grisafi P, Fink GR (1998) EIR1, a root-specific protein involved in auxin transport, is required for gravitropism in Arabidopsis thaliana. *Genes Dev* 12(14):2175–2187.
44. Benková E, et al. (2003) Local, efflux-dependent auxin gradients as a common module for plant organ formation. *Cell* 115(5):591–602.
45. Mravec J, et al. (2008) Interaction of PIN and PGP transport mechanisms in auxin distribution-dependent development. *Development* 135(20):3345–3354.
46. Bennett MJ, et al. (1996) Arabidopsis AUX1 gene: A permease-like regulator of root gravitropism. *Science* 273(5277):948–950.
47. Blakeslee JJ, et al. (2007) Interactions among PIN-FORMED and P-glycoprotein auxin transporters in Arabidopsis. *Plant Cell* 19(1):131–147.
48. Baiges I, Schäffner AR, Affenzeller MJ, Mas A (2002) Plant aquaporins. *Physiol Plant* 115(2):175–182.
49. Ding Z, et al. (2011) Light-mediated polarization of the PIN3 auxin transporter for the phototropic response in Arabidopsis. *Nat Cell Biol* 13(4):447–452.
50. Blilou I, et al. (2005) The PIN auxin efflux facilitator network controls growth and patterning in Arabidopsis roots. *Nature* 433(7021):39–44.
51. Tamura K, et al. (2003) Why green fluorescent fusion proteins have not been observed in the vacuoles of higher plants. *Plant J* 35(4):545–555.
52. Jelinková A, et al. (2010) Probing plant membranes with FM dyes: Tracking, dragging or blocking? *Plant J* 61(5):883–892.
53. Geldner N, Friml J, Stierhof Y-D, Jürgens G, Palme K (2001) Auxin transport inhibitors block PIN1 cycling and vesicle trafficking. *Nature* 413(6854):425–428.
54. Wang J, Cai Y, Miao Y, Lam SK, Jiang L (2009) Wortmannin induces homotypic fusion of plant prevacuolar compartments. *J Exp Bot* 60(11):3075–3083.
55. Sun T-P, Goodman HM, Ausubel FM (1992) Cloning the Arabidopsis GA1 locus by genomic subtraction. *Plant Cell* 4(2):119–128.
56. Cutler SR, Ehrhardt DW, Griffiths JS, Somerville CR (2000) Random GFP:cDNA fusions enable visualization of subcellular structures in cells of Arabidopsis at a high frequency. *Proc Natl Acad Sci USA* 97(7):3718–3723.
57. Swarup R, et al. (2004) Structure-function analysis of the presumptive Arabidopsis auxin permease AUX1. *Plant Cell* 16(11):3069–3083.
58. Paciorek T, Sauer M, Balla J, Wiśniewska J, Friml J (2006) Immunocytochemical techniques for protein localization in sections of plant tissues. *Nat Protoc* 1(1):104–107.